Cell

The Spatial Arrangement of Chromosomes during Prometaphase Facilitates Spindle Assembly

Valentin Magidson,[1,4] Christopher B. O'Connell,[1,4] Jadranka Lončarek,[1] Raja Paul,[2,5] Alex Mogilner,[2] and Alexey Khodjakov[1,3,*]
[1]Wadsworth Center, New York State Department of Health, Albany, NY 12201-509, USA
[2]Department of Neurobiology, Physiology, and Behavior and Department of Mathematics, University of California, Davis, CA 95616, USA
[3]Rensselaer Polytechnic Institute, Troy, NY 12180, USA
[4]These authors contributed equally to this work
[5]Present address: Indian Association for the Cultivation of Science Jadavpur, Kolkata 700032, India
*Correspondence: khodj@wadsworth.org
DOI 10.1016/j.cell.2011.07.012

SUMMARY

Error-free chromosome segregation requires stable attachment of sister kinetochores to the opposite spindle poles (amphitelic attachment). Exactly how amphitelic attachments are achieved during spindle assembly remains elusive. We employed photoactivatable GFP and high-resolution live-cell confocal microscopy to visualize complete 3D movements of individual kinetochores throughout mitosis in nontransformed human cells. Combined with electron microscopy, molecular perturbations, and immunofluorescence analyses, this approach reveals unexpected details of chromosome behavior. Our data demonstrate that unstable lateral interactions between kinetochores and microtubules dominate during early prometaphase. These transient interactions lead to the reproducible arrangement of chromosomes in an equatorial ring on the surface of the nascent spindle. A computational model predicts that this toroidal distribution of chromosomes exposes kinetochores to a high density of microtubules which facilitates subsequent formation of amphitelic attachments. Thus, spindle formation involves a previously overlooked stage of chromosome prepositioning which promotes formation of amphitelic attachments.

INTRODUCTION

The goal of mitosis is to ensure that daughter cells inherit identical genetic information transmitted in the form of duplicated chromosomes. To achieve this goal, cells employ a microtubule-based molecular machine termed the "spindle." Chromosomes attach to spindle microtubules via kinetochores, discrete macromolecular assemblies that reside at the chromosome's centromere. The two kinetochores on each chromosome must stably attach to the opposite spindle poles (amphitelic attachment, reviewed in Walczak et al., 2010).

The general principle of mitotic spindle assembly is described as microtubule "search & capture" (S&C) (Kirschner and Mitchison, 1986). In this model, dynamic plus ends of microtubules grow and shrink until they are captured and stabilized by a kinetochore. Modern computational models predict that unbiased S&C would require hours before each of the kinetochores on 46 chromosomes present in a typical human cell encounters a single microtubule (Wollman et al., 2005). However, mitosis takes less than 30 min in diploid human cells (Yang et al., 2008). This discrepancy implies that additional mechanisms facilitate mitotic spindle assembly by guiding microtubules growth toward kinetochores (O'Connell et al., 2009; Wollman et al., 2005) and/or positioning chromosomes to the areas with high density of microtubules (Kapoor et al., 2006; Lénárt et al., 2005; Paul et al., 2009). To what extent various accessory pathways are harnessed by chromosomes during normal mitosis remains unknown.

Computational models predict that the efficiency of S&C is profoundly affected by geometric constraints such as the shape of the cell and initial positions of centrosomes and chromosomes at the onset of mitosis (Paul et al., 2009). Interestingly, a common feature of mammalian cells is that they round up during division so that the spindle assembles in three-dimensional (3D) space. Yet, owing to technical limitations, most studies of spindle assembly rely on 2D recordings of a single focal plane. Here we report a 3D analysis of centrosome and kinetochore movements in the nontransformed diploid human cell line RPE1. Our data reveal that spindle assembly is facilitated by a transient arrangement of chromosomes in a ring surrounding the central part of the spindle during early prometaphase. Formation of the chromosome ring is driven by the combination of labile lateral kinetochore/microtubule interactions and spindle ejection forces. As a result, centromeres become prepositioned near the spindle equator where kinetochores are exposed to the high density of microtubules that promotes formation of stable amphitelic attachments.

RESULTS

The Pattern of Spindle Elongation and Orientation

The length and orientation of the spindle are determined by spatial separation of the duplicated centrosomes. This separation can occur during prophase or after nuclear envelope breakdown (NEB), during prometaphase (Mole-Bajer, 1975; Roos, 1973). In the latter case the spindle was reported to form as a monopolar structure that subsequently bipolarizes. The "prophase" and "prometaphase" pathways (Mole-Bajer, 1975; Whitehead et al., 1996) were observed in a variety of cell types (Roos, 1973; Toso et al., 2009), and these different routes of centrosome separation may affect the efficiency of spindle assembly (Rosenblatt, 2005; Toso et al., 2009).

To establish the pattern of centrosome separation in RPE1 cells, we recorded 4D movies (Z series spanning the cell volume at every time point). The data were collected at high spatial (1.4 N.A., 0.5 μm Z steps) and temporal (5 s intervals) resolution. Our analyses reveal that centrosomes always separate to the opposite sides of the nucleus prior to NEB in RPE1 cells (Figure 1). In the majority of late-prophase cells (~73%, 49/67), one centrosome resides above and one below the nucleus so that upon NEB, the forming spindle is initially oriented vertically (the angle between the spindle axis and the surface of the coverslip exceeds 30°). Hereafter we refer to these cells "V-cells." In the remaining ~27% (18/67) of cells, centrosomes are separated to the opposite sides of the nucleus horizontally so that spindle axis at NEB is tilted less than 30° with respect to the coverslip (hereafter "H-cells"). In planar XY view, vertical separation of centrosomes in V-cells may create an impression that the centrosomes form a common complex. However, as evident from 3D microscopy, the centrosomes in V-cells are in fact physically separated by the intervening nucleus (Figure 1A; Movie S1 available online).

Due to the disk-like shape of the nucleus, intercentrosome distances at NEB are much greater in H- than in V-cells, and this distance begins to increase immediately after NEB (Figures 1B and 1C). The rate of spindle elongation is not linear with the velocity increasing gradually to 2.2 ± 0.5 μm/min, which is generally consistent with the velocity of antiparallel sliding of microtubules driven by kinesin-5 (Kapitein et al., 2005; Uteng et al., 2008). Although maximal rate of spindle elongation is similar between V- and H-cells (2.3 ± 0.4 and 1.9 ± 0.5 μm/min, Figures 1B′ and 1C′), the peak velocity is reached ~5 min after NEB in V-cells and ~2.5 min in H-cells when the spindle length is ~10 μm in both cases. This suggests that the initial slower phase of spindle elongation is not due to a gradual activation of mitotic kinesins (Blangy et al., 1995; Cahu et al., 2008; Goshima and Vale, 2005). Instead, the elongation rate is likely to reflect changes in the region of antiparallel microtubule overlap.

Because at NEB the centrosomes are already farther apart in H-cells (7.9 ± 2.3 μm), the spindle reaches its full length (13.4 ± 1.2 μm) more rapidly in H- versus V-cells (~5 min versus ~8 min in V-cells; Figures 1B and 1C). In V-cells spindle elongation is concurrent with spindle rotation at the average rate of 6–7 degrees per min, so that ~8 min after NEB the spindle is oriented parallel to the coverslip surface (Figure 1B″, Movie S1). The final orientation of the spindle is identical in V- and H-cells (81.8 ± 6.6° and 82.4 ± 6.9°, respectively; Figures 1B″ and 1C″). Therefore, we conclude that RPE1 cells rely exclusively on the prophase pathway of centrosome separation, and the efficiency of spindle assembly does not depend on the direction of the initial centrosome separation. Our data also reveal the remarkable consistency of spindle assembly in RPE1 cells—in all cells the spindle is fully elongated and properly oriented ~8 min after NEB.

Chromosomes Reproducibly Arrange in a Ring around the Spindle during Early Prometaphase

We used 3D time-lapse movies of the RPE1 cell coexpressing centrin1-GFP and CENP-A-GFP fusions to explore whether there is a specific pattern in the spatial arrangement of chromosomes during the initial stages of spindle formation. Restricting image acquisition to a single channel allowed us to avoid significant photodamage although the centrioles and kinetochores could still be easily discerned in the recordings due to their dramatically different behaviors.

Shortly after NEB, kinetochores residing in the inner parts of the nucleus are rapidly expelled from the central part of the early spindle. This outward movement of the centrally located kinetochores, combined with the inward movement of more peripheral kinetochores, leads to the arrangement of the chromosomes in a ring with the arms pointing outwards and the centromeres inwards toward the spindle axis (Figure 2A, 1:40; Movie S2). This ring forms in both V- and H-cells, although it can be easily overlooked in the conventional xy view due to unfavorable spindle orientation. The ring becomes apparent when viewed along the spindle axis (Figure 2A, 5:30; also see Figure S2). Fixed-cell immunofluorescence analysis confirms that the space inside the chromosome ring is filled with microtubules comprising the compact spindle that forms following NEB (Figures 2B and 2C). The effects of occlusion by the dense network of microtubules are clearly seen in 3D reconstructions (Figures 2B′–2E′ and Movie S3). At later stages of spindle formation, chromosomes move into the central part of the spindle so that the toroidal distribution of kinetochores gradually converts into a typical metaphase plate with evenly spaced kinetochores (Figure 2A, 10:50). The chromosome ring is not unique to RPE1 cells. Similar patterns form during mitosis in transformed human cells (HeLa; Figure S1) as well as in cells originating from other species (rat NRK-52E; Figure S1). A similar arrangement also exists during meiosis in the mouse (Kitajima et al., 2011 [this issue of *Cell*]).

To gain deeper insight into the organization of the chromosome ring, we employed correlative light/electron microscopy (Figure 3 and Figure S2). Serial-section reconstruction of an RPE1 cell fixed during early prometaphase reveals that spindle microtubules densely populate the central part of the nascent spindle between the centrosomes. Interestingly, there is a sharp demarcation in the density of microtubules with only few microtubules protruding beyond the spindle proper (Figure 3B). Most centromeres reside at the boundary of the spindle with their kinetochores interacting with microtubules in a lateral fashion (Figure 3C). Surprisingly, centromeres can be markedly stretched even when both sister kinetochores lack proper end-on microtubule attachments (Figure 3D). This observation is surprising as it is generally assumed that stable amphitelic attachments are required for centromere stretching (reviewed in Maresca and Salmon, 2010; Nezi and Musacchio, 2009).

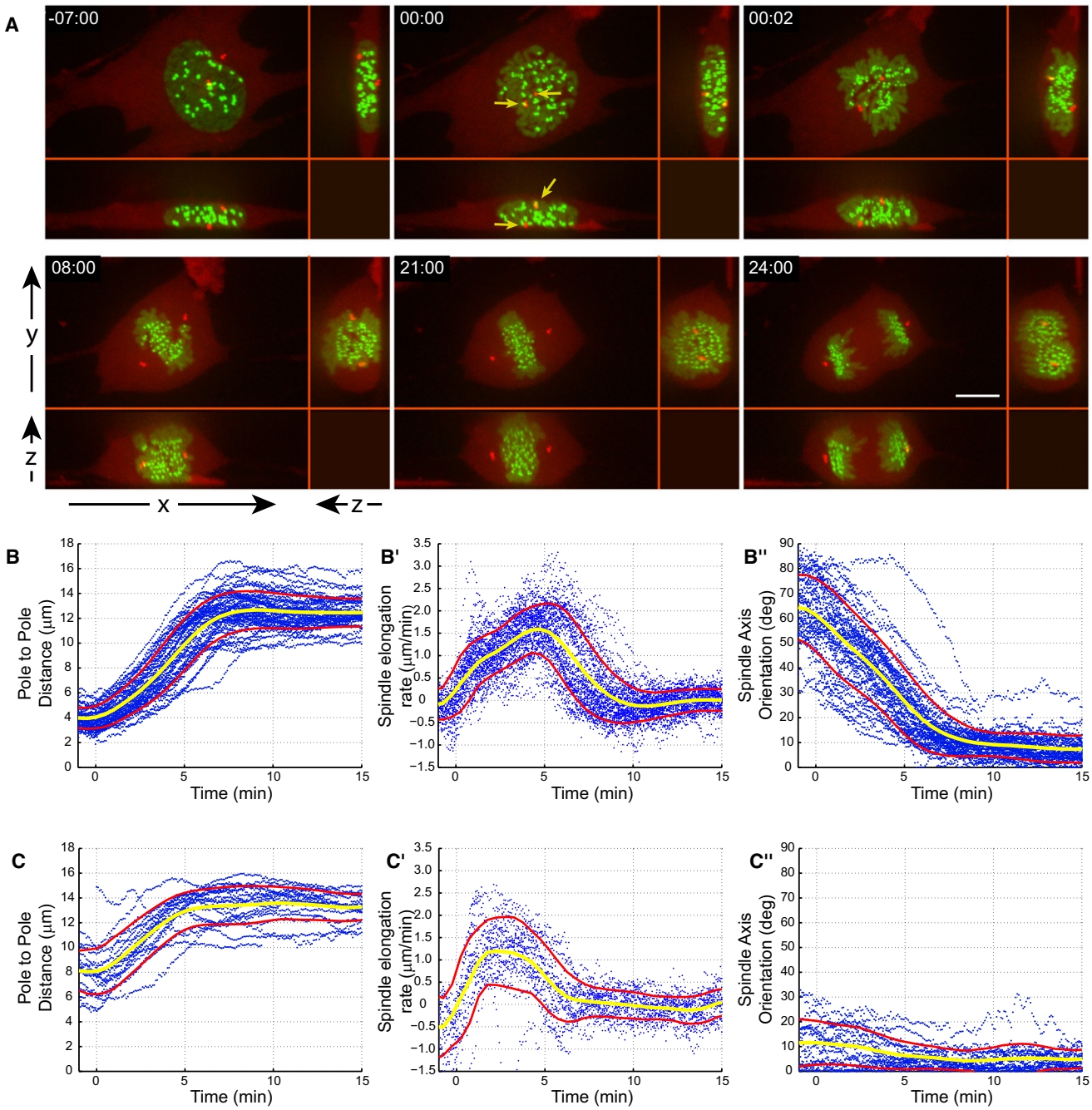

Figure 1. The Pattern of Spindle Elongation and Orientation in RPE1 Cells

(A) An RPE1 cell expressing CENP-A-GFP (green) to label the kinetochores and centrin1-tdTomato (red) to label the centrosomes is shown. Although in xy view the centrosomes appear to reside in a common complex just before NEB (arrows in 00:00), xz and yz views demonstrate that the centrosomes are actually positioned on the opposite sides of the nucleus (above and below).

(B and C) Numeric characterization of spindle elongation and orientation in 67 RPE1 cells coexpressing centrin-GFP and CENP-A-PAGFP. Each plot presents individual trajectories (blue dots), the average value (yellow line), and standard deviation (SD) (red lines). Spindle length (B and C), rate of spindle elongation (B′ and C′), and spindle orientation (B″ and C″) in V- (B–B″) versus H-cells (C–C″). Note the remarkable reproducibility of spindle elongation and rotation pattern.

The Chromosome Ring Accelerates Mitotic Spindle Assembly

Having observed reproducible formation of the chromosome ring during mitosis, we sought to establish whether this pattern bears a functional significance for spindle assembly. To this end, we harnessed the computational model constructed by Paul and coworkers (2009), which predicted that only a few kinetochores would be initially exposed to microtubules in the

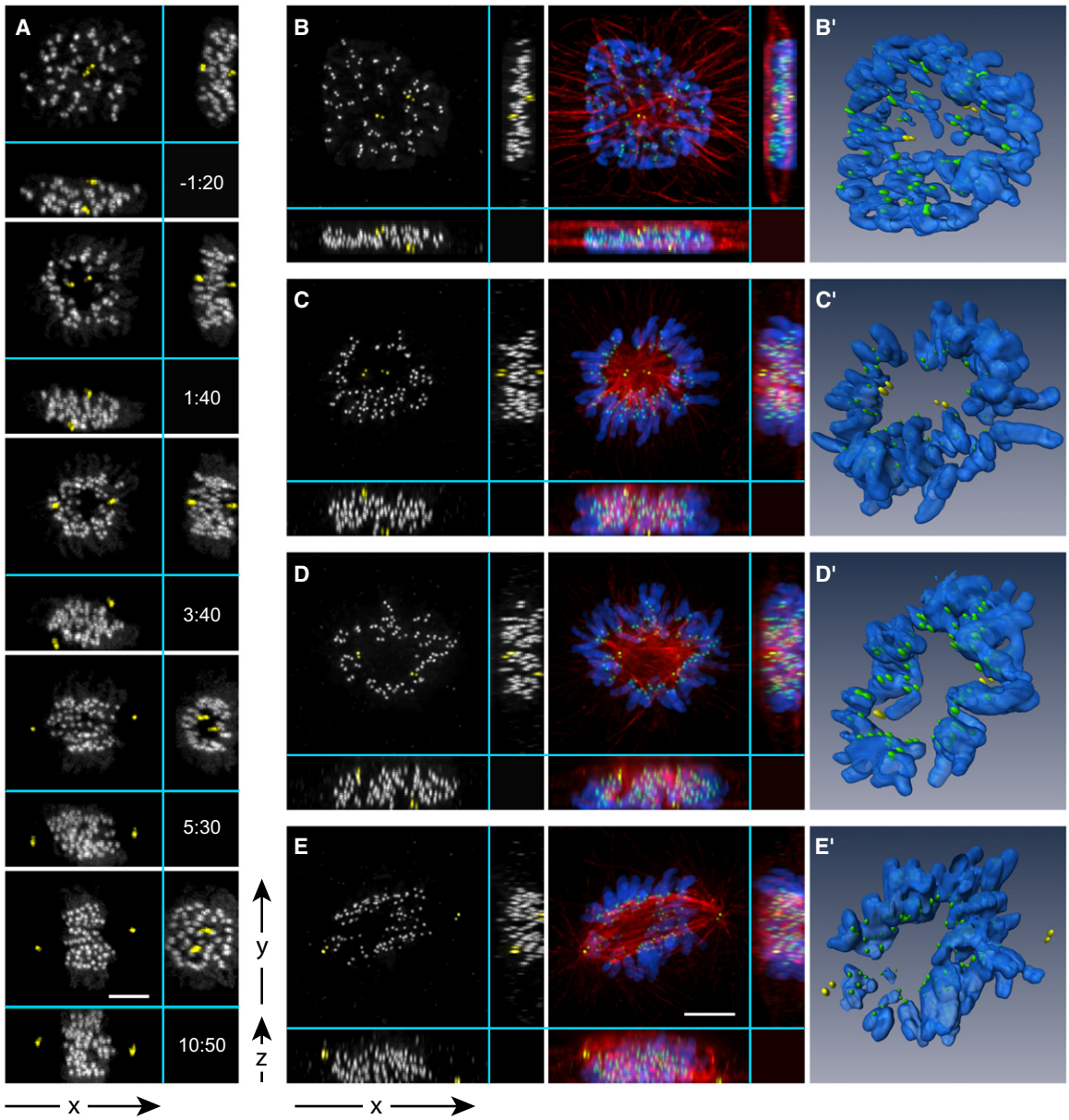

Figure 2. Multidimensional Analysis of Spindle Assembly

(A) Selected frames from a high-resolution 4D time-lapse movie of a cell labeled with centrin1-GFP and CENP-A-GFP. For clarity, centrioles are pseudocolored yellow. Notice that one centrosome is positioned above and the other below the nucleus (V-cell). In less than 2 min after NEB a clear zone, void of chromosomes, develops between the separating centrosomes (1:40). As the spindle rotates, the zone persists as evident from the yz view (5:30). Later, the chromosomes repopulate the central part of the spindle (10:50). Time shown relative to NEB in min:s.

(B–E) Immunofluorescence images and computer-generated surface renderings (B′–E′) of fixed RPE1 cells during early-to-mid prometaphase. The volume between the poles that is void of chromosomes is filled with a high density of microtubules (C– D; C′–D′; See also Figure S1). Once the spindle rotates to a vertical position, a typical prometaphase morphology becomes apparent in the conventional xy view (E and E′). Bars, 5 μm.

crowded environment of a human cell with 46 chromosomes. To estimate whether formation of the chromosome ring would facilitate S&C within the constraints of the Paul model, two types of simulations were conducted. The chromosomes were assumed to either be spread uniformly and randomly throughout the nuclear space (oblate spheroid with 14 × 14 × 7 μm) or form a toroid with the dimensions extracted from our live- and fixed-cell observations (inner radius 4 μm and outer radius 7 μm). Although the difference between these two types of chromosome distribution is visually subtle (cf. Figure 4A, ''Random'' versus ''Toroidal''), the simulation predicts that the efficiency of S&C is significantly improved by the chromosome ring. The number of kinetochores exposed to microtubules increases from ~30% in the case of uniformly distributed chromosomes

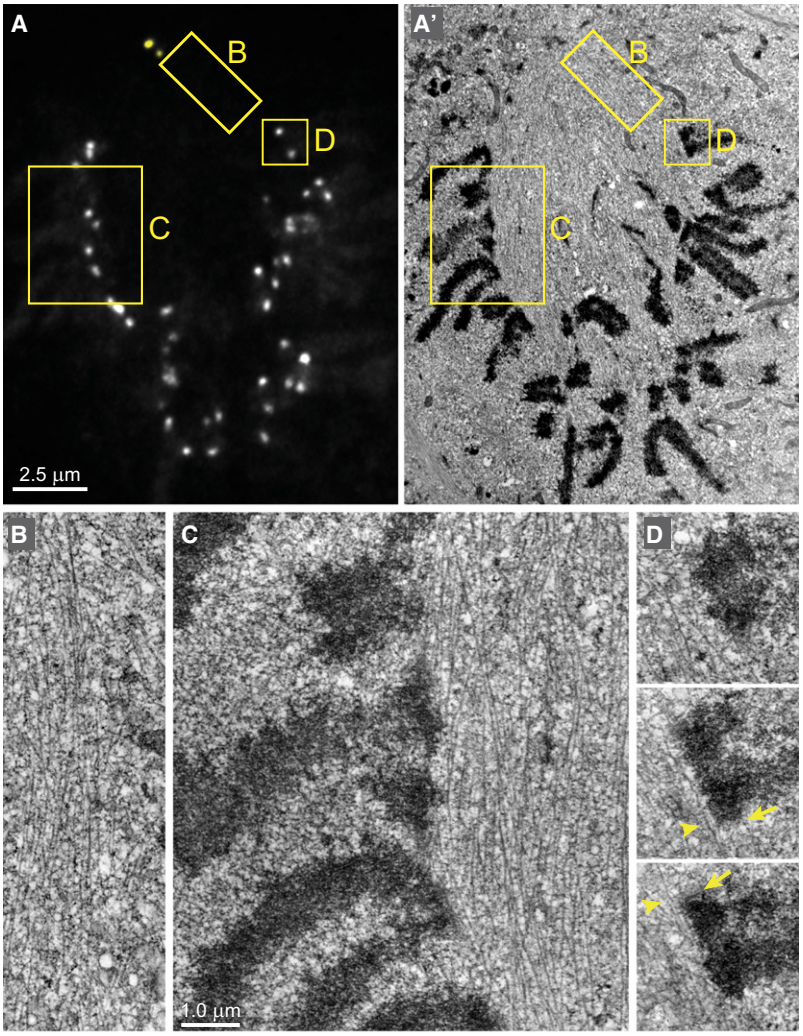

Figure 3. Architecture of the Early Prometaphase Spindle

(A and A′) A single GFP-fluorescence focal plane (A) and the corresponding EM section (A′) selected from complete 3D datasets. Chromosomes are excluded from the spindle and the centromeres reside on the spindle surface. Insets denote the areas presented at higher magnification in (B)–(D).

(B) A view of the sharp demarcation between the spindle and the rest of the cytoplasm showing the high density of microtubules inside the spindle and their absence in the cytoplasm.

(C) The centromeres reside on the surface of the spindle. Note that only few microtubules can be found outside the spindle between the chromosome arms.

(D) Serial sections through a centromere on the surface of the spindle. Both sister kinetochores (arrows) lack end-on microtubule attachments but laterally interact with individual microtubules (arrowheads) that run parallel to the centromere. The distance between sister kinetochores is ~1 μm in spite of the lack of end-on attachments.

See Figure S3 for 3D data on the kinetochore distribution in this cell. Scale bars are 2.5 μm for (A) and (A′) and 1 μm for (B)–(D).

to ~70% in the ring configuration. As a result, within a 3 min long search, ~60% of the chromosomes would be captured and incorporated into the spindle in the ring configuration, which is a dramatic improvement over the randomly distributed chromosomes. Thus, formation of the chromosome ring at the onset of mitosis is advantageous for S&C and is predicted to accelerate mitotic spindle assembly by approximately 6–8 min.

To experimentally test this prediction, we followed the dynamics of mitosis in cells depleted of the chromokinesin Kid (kinesin-10) (Tokai et al., 1996). We reasoned that expulsion of chromosomes from the central part of the spindle is likely to be driven by the spindle ejection force (Rieder et al., 1986), which is primarily generated by Kid (Levesque and Compton, 2001). Previous studies have established that inactivation of Kid does not prevent formation of a functional bipolar spindle, although several aspects of chromosome movement are affected and the duration of mitosis is increased (Levesque and Compton, 2001; Tokai-Nishizumi et al., 2005). Our 3D recordings reveal that, in fact, formation of the chromosome ring is inhibited upon siRNA depletion of Kid (Figure 4B), and the duration of mitosis increases by approximately 6 min (from 19.4 ± 2.9 min in control [n = 8] to 25 ± 3.3 min in Kid-depleted cells [n = 10]), which is in excellent agreement with the model. The delay is due to slower formation of the metaphase plate (cf. Figures 4B and 4C; Movie S4 and Movie S5). We also observed similar inhibition of the ring formation and prolongation of prometaphase in cells microinjected with an antibody raised against the Kid DNA-binding domain, which was previously used by Levesque and Compton (2001) (n = 4; data not shown). Thus, experimental perturbation of chromosome ring formation decreases the efficiency of spindle assembly as predicted by the computational model.

The Pattern of Chromosome Movements

Three-dimensional recordings of cells with GFP-tagged kinetochores and centrioles allowed us to visualize the general pattern of spindle assembly. However, owing to the large number of chromosomes and complexity of their movements in 3D space, we were unable to continuously follow trajectories of individual chromosomes from NEB through anaphase in these recordings. To overcome this limitation, we developed an assay in which one or two pairs of sister kinetochores were photoactivated in RPE1 cells expressing CENP-A-PAGFP (Figure S3A). Photoactivation was conducted with pulses of highly focused 405 nm laser light during late G2 or early prophase before the chromosomes were fully condensed. This ensured that selection of chromosomes was not biased toward particular sizes of chromosomes or their location with respect to the centrosomes because the exact position of centrosomes during NEB could not be predicted at the time of photoactivation. Due to a low number of objects in

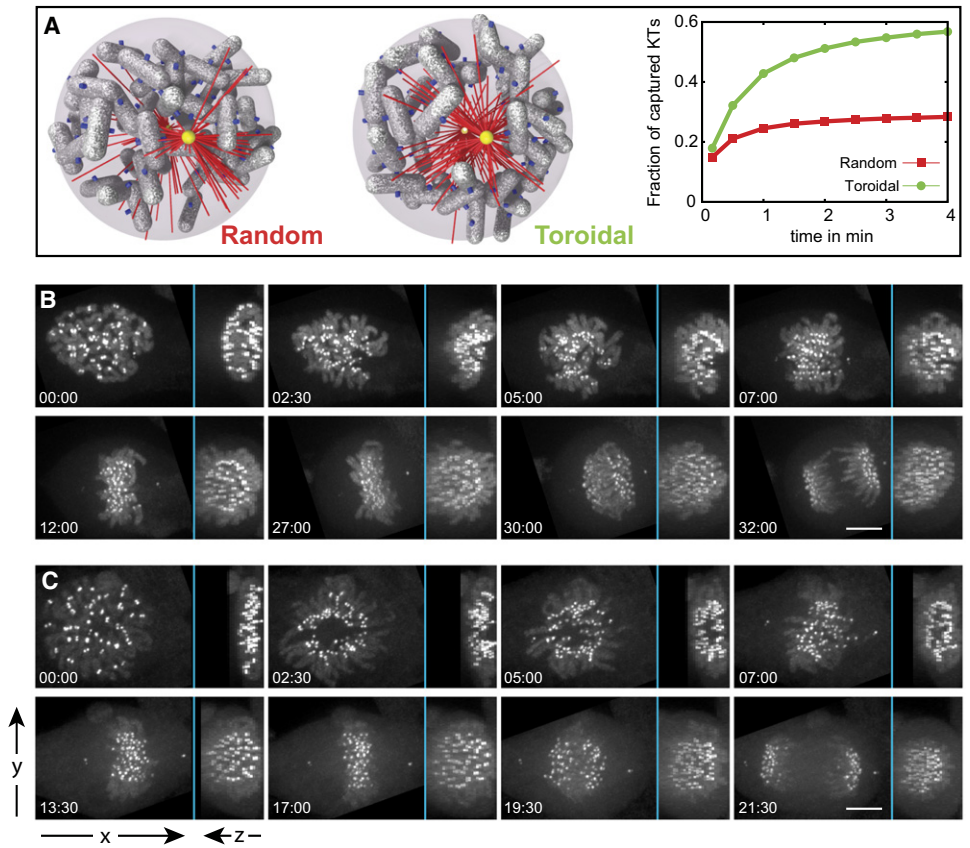

Figure 4. The Chromosome Ring Facilitates Spindle Assembly

(A) Two types of initial chromosome distribution (random and toroidal) and corresponding dynamics of kinetochore capture predicted in our computer simulations. The toroidal distribution provides a clear kinetic advantage.

(B and C) Mitosis in chromokinesin Kid-depleted (B) versus control (C) cells. Depletion of Kid inhibits formation of the central clear zone. In contrast, chromosomes in control cells are excluded from the center of the spindle during early prometaphase (C; 02:30–07:00). Notice that to generate consistent perspective, both sequences are illustrated by maximal-intensity projections that are perpendicular (left part of each frame) and parallel (right part) to the spindle axis during metaphase.

our recordings (1–2 pairs of kinetochores and 2 centrosomes), 3D positions of sister kinetochores and centrosomes can be reliably tracked and analyzed (Figures S3B and S3C; Movie S6). Comparative and averaging analyses of 81 trajectories (50 from NEB through anaphase and 31 from NEB through metaphase) obtained in 67 cells allowed us to identify characteristic features of chromosome behavior in diploid human cells (Figure S3D). In turn, these features help to reveal the pathways that are prevalent during normal spindle assembly.

Consistent with data obtained in cells with all kinetochores labeled, individual-kinetochore tracking reveals that most centromeres remain near the spindle equator from NEB through anaphase onset (AO). Typically, the distance between kinetochores and spindle poles increases gradually during prometaphase (Figure 5A and Figure S3) until it reaches its maximum of 6.7 ± 1.6 μm ~8 min after NEB when the prometaphase centrosome separation is completed (Figure S3D). Thus, somewhat counterintuitively, during spindle assembly the total displacement of centrosomes from their positions at NEB is greater than the total displacement of a typical chromosome.

At the spindle equator, some chromosomes undergo continuous oscillations throughout metaphase, other chromosomes remain motionless, and some switch between periods of oscillations and irregular movements (Figure 5A). To characterize these behaviors numerically we used the DAP (deviation from average position) criterion developed by Stumpff and coauthors (2008). We determined DAP for every chromosome in a series of 5 min windows that span from late prometaphase to AO. Chromosomes with DAP > 0.4 were considered oscillating (Stumpff et al., 2008). As shown in Figure 5B, 28% of chromosomes oscillate continuously, 68% undergo transitions between periods of oscillations and relative motionless, and 4% remain motionless throughout metaphase. The reason(s) for this variable behavior of congressed chromosomes, which are all expected to continuously maintain amphitelic attachments, remain unknown. We noticed that regular oscillations always begin after the centromere becomes stretched to ~1 μm, which is consistent with the notion that oscillating chromosomes are stably attached to microtubules in the end-on fashion (Jaqaman et al., 2010). However, achieving the full

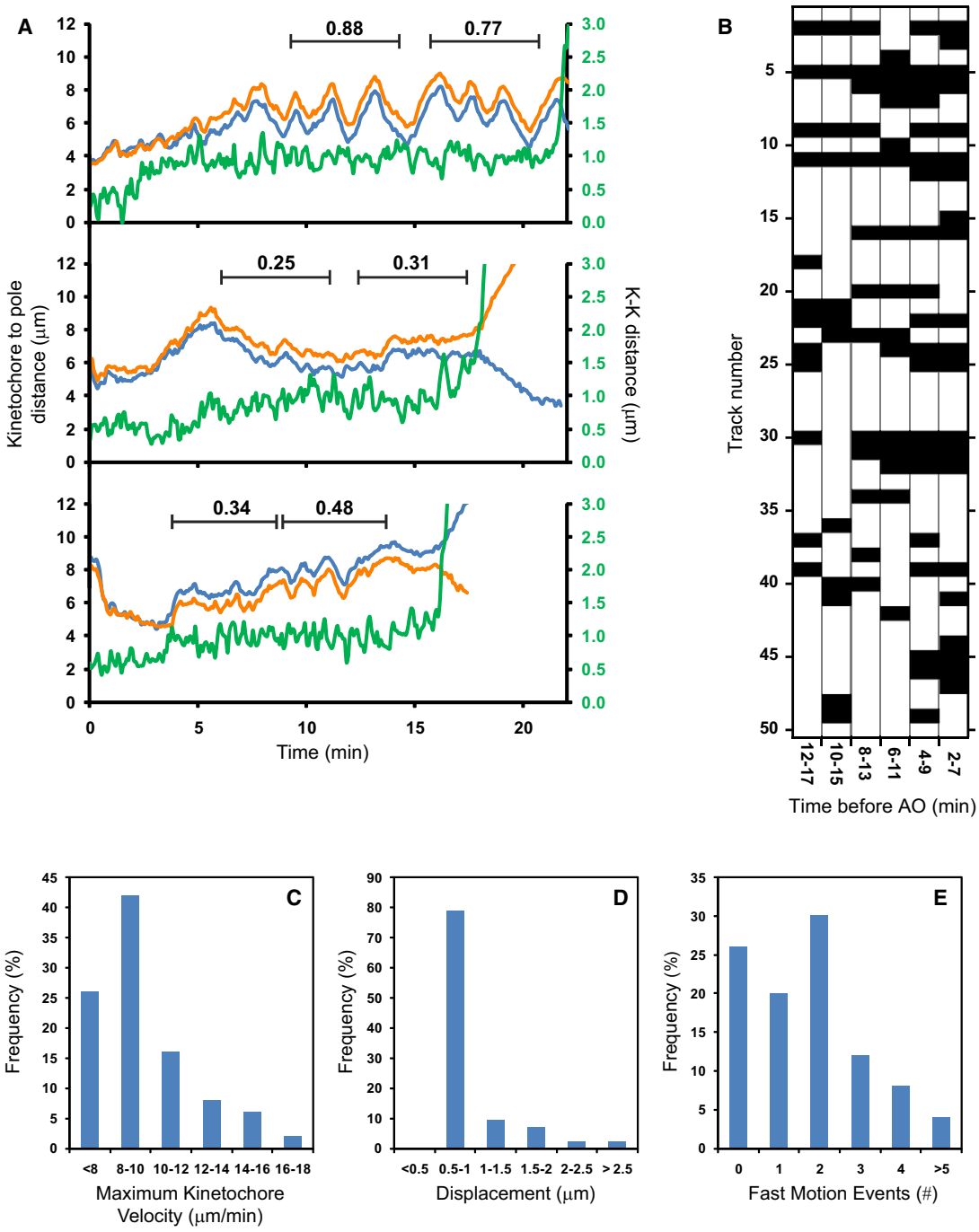

Figure 5. Chromosome Movements during Prometaphase and Metaphase

(A) Examples of individual chromosome behavior. The plots present changes in the distances between one spindle pole and each photoactivated kinetochore in a sister pair (orange and blue lines) as well as centromere stretch (green) from NEB through AO. One chromosome (top) exhibits oscillatory behavior, another chromosome remains relatively motionless during metaphase (middle), whereas the third chromosome switches between periods of oscillation and irregular movements (bottom). Deviation from average position (DAP) values are shown for periods marked by black lines.

(B) Summary of oscillatory behavior for 50 individual chromosomes. Black blocks represent DAP < 0.4 (nonoscillating behavior); white blocks correspond to DAP values exceeding 0.4 (oscillation).

(C) Histogram of maximum velocity reached by kinetochores.

(D) Displacements resulting from rapid (>8 μm/min) kinetochore movements.

(E) Number of rapid kinetochore movements exhibited by individual chromosomes.

See also Figure S3.

stretch of the centromere is not sufficient to induce oscillation (Figure 5A).

Another characteristic chromosome behavior that was originally described in extremely flat newt lung cells is the rapid (~18 μm/min) gliding of the kinetochore along the captured microtubule toward the centrosome (Rieder and Alexander, 1990; Skibbens et al., 1993). This movement displaces the chromosome by ~10 μm on average (Skibbens et al., 1993). Rapid centromere gliding (~10 μm/min) has also been observed in human U2-OS cells. However, in single-focal plane recordings, it appears to affect less than 20% of chromosomes (Yang et al., 2008). Our analyses of chromosome movements in 3D reveal that ~75% of kinetochores in RPE1 cells exceed momentous velocity of 8 μm/min at least once during the course of prometaphase and metaphase. Higher velocities up to 18 μm/min are also observed, but at progressively lower frequencies (Figure 5C). The periods of rapid movement are brief (5–15 s), resulting in the average displacement of 0.93 ± 0.44 μm, although in rare cases the centromere displaces up to 3 μm (Figure 5D). An individual chromosome can undergo several rapid movements (Figure 5E), which indicates that the initial interactions with microtubules often do not result in a stable attachment of the kinetochore. Whereas the majority of the rapid movements (~60%) are observed within 5 min after NEB, some (~10%) can occur 5–10 min before AO when the metaphase plate is already fully formed.

Surprisingly, most rapid kinetochore movements are not directed toward one of the centrosomes. As evident from the plot presented in Figure S3C (arrows), fast movement can lead to a simultaneous decrease of the distances between the centromere and both centrosomes to a similar extent, indicating that the chromosome moves to a position located near the middle of the nascent spindle. We used the ratio of kinetochore displacement toward different centrosomes to characterize the predominant direction of fast movement. This ratio is negative when the movement is directed toward one centrosome and away from the other. For centromeres that move toward both centrosomes to the same extent, the ratio is 1. This metric reveals that ~50% of fast kinetochore movements (n = 65) during early prometaphase are directed to center of the spindle with the ratios between 0.5 and 1.5 (standard deviation [SD] = 0.25).

Together, these observations suggest that during spindle formation unattached kinetochores in RPE1 cells experience frequent albeit transient lateral interactions with spindle microtubules. These interactions do not result in a significant repositioning of the chromosome, and only some of these interactions lead to a stable attachment.

Lateral Interactions between Kinetochores and Microtubules Pre-position and Orient Centromeres to Foster Formation of Stable End-On Attachments

Thus far our experiments reveal that during early prometaphase centromeres become positioned on the surface of the nascent spindle where the high density of microtubules results in numerous lateral interactions with the unattached kinetochores. To identify the aspects of spindle assembly that depend upon these lateral interactions during normal mitosis, we compared the behavior of chromosomes in normal and Nuf2-depleted RPE1 cells. siRNA depletion of Nuf2, an NDC80-complex protein, has been shown to preclude formation of end-on microtubule attachments without significantly affecting lateral interactions (DeLuca et al., 2005). In fact, chromosomes can congress to a typical metaphase plate in cells codepleted for Nuf2 and HSET (Cai et al., 2009). Three-dimensional recordings in RPE1 cells with all kinetochores labeled via CENP-A-GFP expression demonstrate that the chromosome ring forms in Nuf2-depleted cells and it tends to persist longer than in untreated cells (Figure S4).

Tracking individual photoactivated kinetochore pairs demonstrates that immediately prior to NEB, the average distances between sister kinetochores are somewhat smaller in Nuf2-depleted (0.33 ± 0.14 μm) than in control RPE1 cells (0.45 ± 0.22 μm). During prometaphase these distances increase gradually until they reach plateaus approximately 10 min after NEB in both control and Nuf2-depleted cells (Figures 6A and 6B). In agreement with previous studies (Cai et al., 2009; DeLuca et al., 2002), on average centromere stretching is greater by ~40% in controls (0.96 ± 0.21 μm) than in Nuf2-depleted cells (0.62 ± 0.2 μm) during late prometaphase. However, an important outcome of our time-resolved analysis is that even in the absence of end-on attachments interkinetochore distances progressively increase during early prometaphase. We also find the distribution of interkinetochore distances in Nuf2-depleted cells to be similar to that in control cells during early prometaphase when the chromosome ring is most prominent (Figure S4C). This similarity is consistent with the notion that lateral interactions dominate during chromosome ring formation in control cells. Another interesting feature evident in trajectories of individual chromosomes is that transition from the low-stretch to high-stretch state usually occurs gradually over a period of several minutes in both control (Figure 6C; Figure S3C) and Nuf2-depleted cells (Figure 6D), and this transition does not strictly correlate with achieving a stable orientation of the centromere.

In both control and Nuf2-depleted cells, centromeres are randomly oriented with respect to the axis of the forming spindle at NEB. Within the first 10 min of prometaphase, the average angle between the lines connecting the centrosomes and the line connecting sister kinetochores decreases to ~15° in control and ~30° in Nuf2-depleted cells (Figures 6A and 6B, violet). Thus, even in the absence of end-on microtubule attachments, centromeres become roughly oriented with respect to the spindle. However, analysis of chromosome trajectories demonstrates that the orientation of individual centromeres in Nuf2-depleted cells continues to fluctuate between periods of relative stability and ''wobbling'' (Figure 6D). These fluctuations are reflected in the standard deviation from the average angle that remains wide even as the average values gradually improve (Figure 6B). Similar fluctuations are consistently observed during earlier prometaphase in control cells (cf. Figures 6A and 6C). In severe cases, centromeres are seen to undergo a complete revolution so that the kinetochore that initially faces one centrosome becomes oriented toward the other centrosome (Figure 6E and Movie S7). In other instances the original centromere orientation is restored after a period of wobbling. To

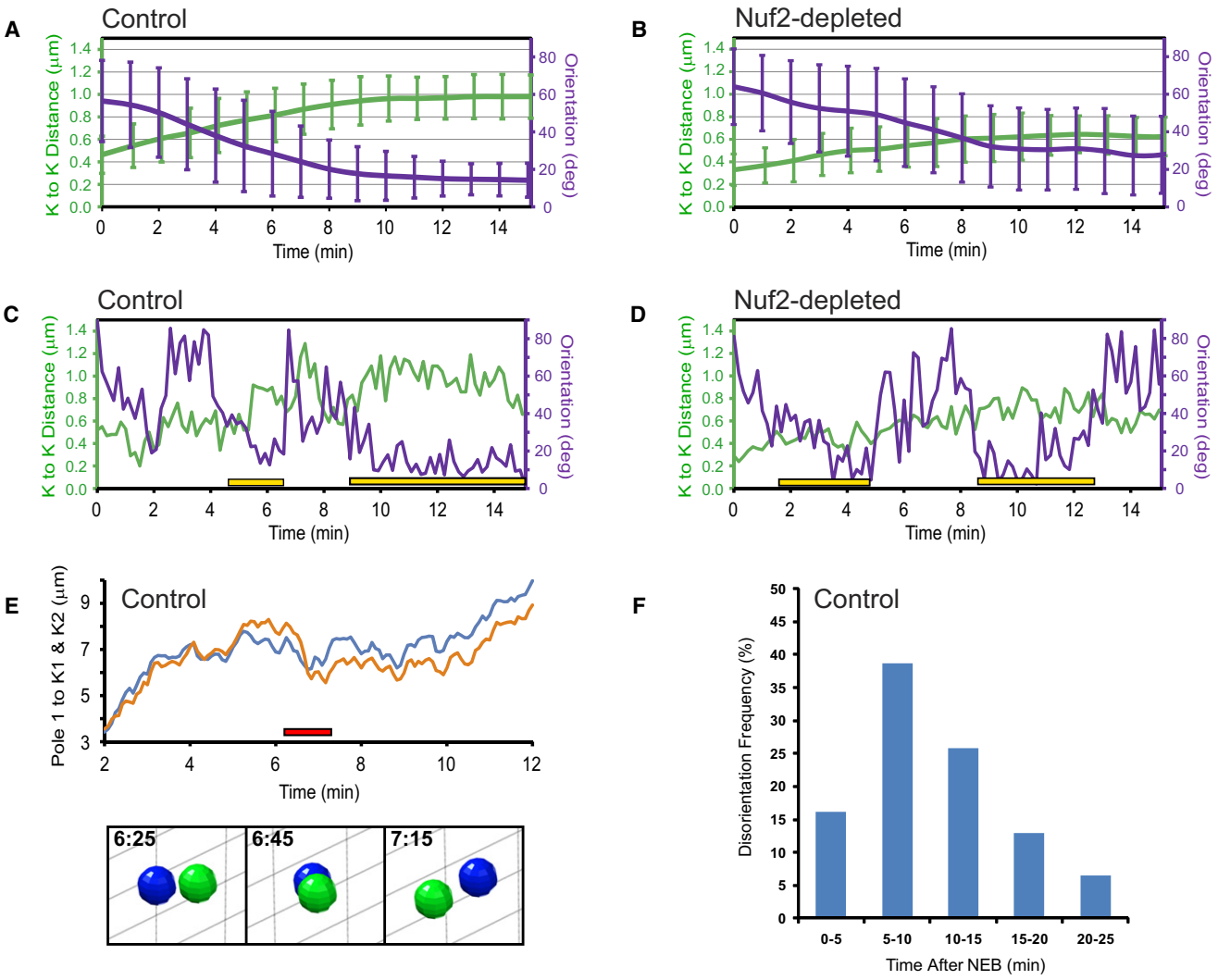

Figure 6. Centromere Stretch and Orientation during Prometaphase

(A and B) Changes in the average value of interkinetochore distance (green lines) and centromere orientation with respect to the spindle axis (violet lines) during the first 15 min after NEB in control (A) and Nuf2-depleted (B) cells. Error bars denote SD. See also Figure S4.

(C and D) Examples of the changes in the interkinetochore distance and centromere orientation in control (C) and Nuf2-depleted (D) cells. Yellow bars denote periods when persistent, proper alignment of the centromere has been achieved. Notice that interkinetochore distances do not change when centromeres become disoriented.

(E) An example of centromere reorientation during normal prometaphase (same kinetochore pair as in C). The kinetochore oriented to the left at 6:25 becomes oriented to the right at 7:15 (images; also see Movie S7). Note that the reorientation occurs when the centromere resides close to the spindle equator.

(F) Frequency of centromere disorientations at different stages of spindle assembly.

quantify the frequency of centromere disorientations, we determined the number of events when a centromere that had remained stably oriented for at least 1 min (12 frames) lost its orientation by tilting more than 45° with respect to the spindle axis. By this criterion, ~42% of chromosomes (21/50) transiently lose their initial orientation, whereas ~33% (7/21) of these chromosomes become disoriented more than once. Centromere disorientations are most frequent during early- to mid-prometaphase (Figure 6F), although a significant number of them (~20%) occur later in mitosis when the metaphase plate is already fully formed (Figure 6F).

Presence of Laterally Attached Kinetochores in a Fully Congressed Metaphase Plate

Our analysis of centromere stretch and orientation support that amphitelic attachment is not required for positioning the chromosome at the spindle equator. To investigate whether all chromosomes inside completely congressed metaphase plates are in fact attached to microtubules in amphitelic fashion, we employed serial-section electron microscopy (EM). By correlating complete 3D light microscopy (LM) and EM datasets, we were able to locate each of the 92 kinetochores in a metaphase cell.

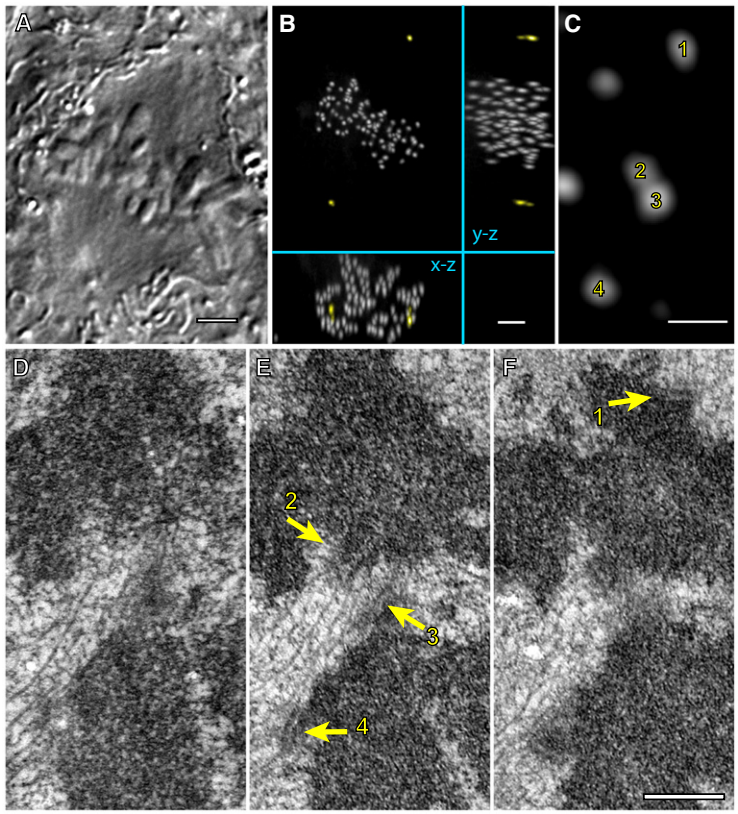

Figure 7. Fully Congressed Chromosomes Can Lack Amphitelic Attachment

DIC image (A) and maximal-intensity xy, xz, and yz projections of GFP fluorescence (B) of a fixed metaphase RPE1 cell expressing centrin1-GFP and CENP-A-GFP.

(C) A higher-magnification view (xy projection) showing two pairs (1–2 and 3–4) of sister chromosomes positioned within the metaphase plate.

(D–F) Serial 70 nm thin sections through the area presented in (C) demonstrate that kinetochores 1, 2, and 4 are attached to microtubules in the end-on fashion, which implies that the chromosome in the top half of the image is amphitelic. In contrast, kinetochore 3 lacks end-on attachment, and it is shielded from the top spindle pole by a mass of chromatin positioned in front of the kinetochore. This kinetochore laterally interacts with microtubules of the K-fiber that terminates within kinetochore 2.

Bars in (A) and (B), 5 μm. Bars in (C)–(F), 0.5 μm.

The reconstructed cell is in late metaphase with all chromosomes fully congressed (Figure 7A), and the kinetochores are uniformly distributed in the central part of the spindle characteristic of late metaphase. Expectedly, most of the 92 kinetochores are properly attached to prominent K-fibers with microtubules terminating within the kinetochore plate (e.g., kinetochores 1, 2, and 4; Figures 7D–7F). However, three chromosomes lack amphitelic attachment. In each of these instances, one sister kinetochore is attached to microtubules in an end-on fashion, whereas the other kinetochore only laterally interacts with microtubules of a K-fiber that terminates in a kinetochore on a different chromosome (kinetochore 3; Figures 7D–7F). This configuration has been previously observed only during congression of monooriented chromosomes but not inside the metaphase plate (Kapoor et al., 2006). It is noteworthy that in two cases the laterally attached kinetochores are completely shielded from one of the spindle poles by arms of other chromosomes. This steric impediment prevents a direct microtubule connection to the spindle pole.

DISCUSSION

Several recent studies demonstrate that the fidelity of chromosome segregation and fate of the progeny depend on the mode of spindle assembly. For example, transient deviations from the bipolar spindle geometry during prometaphase or subtle changes in the stability of kinetochore microtubules have been shown to cause chromosomal instability, although a seemingly normal bipolar spindle forms under these conditions (Bakhoum et al., 2009; Ganem et al., 2009; Silkworth et al., 2009). Exceedingly slow progression through prometaphase arrests the progeny in the ensuing G1 (Uetake and Sluder, 2010). Thus, it is critical to reveal the exact pathways responsible for the timely assembly of the spindle and accurate establishment of proper kinetochore attachments. Our approach of tracking individual spindle components in 3D throughout mitosis allows us to shed new light on this issue. The rationale is that different spindle assembly mechanisms result in distinct chromosome behavior. Thus, contributions of the mechanisms governing normal spindle assembly can be inferred from the analyses of the unique route taken by each chromosome during mitosis.

A major finding of our work presented here is that the majority of chromosomes in normal human cells become instantaneously bioriented (positioned close to the spindle equator) from the onset of mitosis and they remain in this locale until anaphase. Interestingly, centromeres of these bioriented chromosomes frequently wobble, indicating that they have not achieved stable amphitelic attachment. This notion gains support from the EM data that many kinetochores in the middle of the spindle interact with microtubules only in a lateral fashion. Some of these laterally attached kinetochores can even be found in a mature metaphase plate. Although it has been shown that chromosomes can in principle congress in the absence of end-on attachments (Cai et al., 2009), the functional significance of this mechanism remained ambiguous. We find that most chromosomes normally achieve biorientation prior to formation of stable amphitelic attachments, and lateral interactions make a major contribution during normal spindle assembly.

Instantaneous biorientation can only be achieved if both kinetochores reside in an area with extremely high microtubule density and are not shielded by other chromosomes. Such a condition is not possible when chromosomes are randomly distributed in the relatively small space formerly occupied by the nucleus (Paul et al., 2009). The reproducible pattern of

chromosome and centrosome movement observed during early prometaphase provides a straightforward explanation of how the chromosome shielding constraint is overcome.

Arrangement of chromosomes in a ring around the spindle during prometaphase has long been known to exist in a variety of cell types (Chaly and Brown, 1988; Mosgöller et al., 1991), although the functional significance of this distribution remained ambiguous. The ring has been suggested to provide a means for nonrandom distribution of chromosomes into daughter cells (Nagele et al., 1995). However, data indicating that chromosomes are arranged randomly within the ring do not support this hypothesis (Allison and Nestor, 1999).

We find that formation of the ring depends on the spindle ejection force (Rieder and Salmon, 1994), which is mediated by plus-end-directed motor activity of kinesin-10 (Levesque and Compton, 2001). Until now the role of the spindle ejection force remained poorly understood. Originally thought to provide spatial cues for chromosome congression (Khodjakov et al., 1999; Rieder et al., 1986), the spindle ejection force was left without a clear function due to demonstration of normal chromosome congression upon experimental inhibition of the spindle ejection force (Levesque and Compton, 2001). Our data suggest that the spindle ejection force functions to efficiently expel the chromosome arms from the center of the nascent spindle. This, combined with centripetal forces acting on the centromeres, positions the kinetochores on the surface of the nascent spindle where they are exposed to a high density of microtubules from both spindle poles. Consistent with the notion that early prometaphase is dominated by lateral interactions between kinetochores and microtubules, we find that the chromosome ring forms in Nuf2-depleted cells where kinetochores are not capable of stable end-on microtubule attachments.

Assembly of a compact spindle densely packed with microtubules appears to be the key for efficient spindle assembly. The high density of microtubules between the centrosomes is likely to be established initially by the preferential growth of microtubules toward the high concentration of RanGTP inside the volume formerly occupied by the nucleus (O'Connell et al., 2009). In this mechanism, microtubule density would be particularly high within the spindle if at NEB the centrosomes reside on the opposite sides of the nucleus, which according to our 3D recordings occurs in the great majority of RPE1 cells. It would be extremely interesting to determine whether the efficiency of spindle assembly and/or the fidelity of chromosome segregation are compromised in cells that naturally fail to separate the centrosome prior to NEB (see Toso et al., 2009).

In summary, our work reveals a mechanism that facilitates S&C by pre-positioning spindle components so that kinetochores can more easily establish end-on microtubule attachments. This was made possible by two technological breakthroughs: (1) continuous tracking of an individual chromosome from the onset of mitosis to anaphase; (2) following spindle formation in true 3D space at high temporal and spatial resolutions. These advancements allowed us to reconstruct the path taken by a typical chromosome during spindle assembly by averaging the unique trajectories of randomly selected chromosomes. The data presented here establish the baseline of normal chromosome behavior, which will be invaluable in the future examinations of pathological conditions arising from the deficiencies in key proteins involved in mitosis.

EXPERIMENTAL PROCEDURES

Cell Culture and Generation of Stable Cell Lines

RPE1 cells (Clontech) were grown in DMEM supplemented with 10% FCS (Invitrogen) at 37°, 5% CO_2. To generate cells with fluorescent kinetochores and centrosomes, cells were first transfected with CENP-A-PAGFP in LentiLox 3.1. Individual clones selected for the desired expression level were subsequently transfected with centrin1-GFP. This approach allowed us to ensure that the intensity of individual kinetochores after photoactivation was comparable with the intensity of GFP-labeled centrioles. A similar strategy was used to construct RPE1 cells coexpressing GFP-CENP-A + centrin1-GFP, and GFP-CENP-A + centrin1-tdTomato. For high-resolution imaging, cells were grown on glass coverslips to subconfluence and mounted in Rose chambers containing CO_2-independent medium (Invitrogen) supplemented with 10% FCS and antibiotics.

Protein Inactivation

Oligofectamine (Invitrogen) was used for siRNA transfections according to the manufacturer's protocol. Cells were analyzed 36–72 hr after transfection. Target sequences are described elsewhere (Tokai-Nishizumi et al., 2005 for Kid and DeLuca et al., 2002 for Nuf2). Efficiency of siRNA depletions was confirmed by antibody staining (anti-Hec1 antibody was used for Nuf2 depletion). In Nuf2 experiments, only cells that failed to form a tight metaphase plate were analyzed.

Alternatively, Kid was inactivated via microinjection of a function-blocking antibody raised against the DNA-binding domain of the molecule (Levesque and Compton, 2001). The antibody was purified and injected into the nucleus as in Levesque and Compton (2001), except that the injections were conducted during prophase and the antibody concentration in the needle was 16.8 mg/ml.

Photoactivation and Analysis of Kinetochore/Centrosome Trajectories

Individual kinetochore pairs were photoactivated with 405 nm diode laser (OZ-2000, Oz Optics, Ottawa, Ontario). Details of the microscopy workstation and laser coupling are described elsewhere (Magidson et al., 2007). Briefly, the collimated beam was steered through a dedicated epi-port of a Nikon TE-2000E PFS microscope and focused by a 100× Plan Apo, N.A. 1.4 oil immersion objective lens. Images were recorded in spinning-disk confocal mode (CSU-10, Yokogawa, Tokyo, Japan) on a back-illuminated Cascade 512B EM CCD camera (Photometrics). Kinetochores were activated during late G2 or prophase, and the recordings were initialized shortly before nuclear envelope breakdown. Seventeen focal planes at 0.5 μm Z steps were recorded at each time point.

To decrease unnecessary exposure of cells to light, we introduced a shutter override into automatic image acquisition. In those instances when centrosomes and kinetochores were positioned at similar depth, excitation light was blocked once in-focus images of all objects had been recorded. Details of this approach are presented elsewhere (V.M., J.L., and A.K., unpublished data).

Determining complete 3D coordinates requires that the objects do not overlap in two of the three possible orthogonal projections (xy, xz, and yz). Due to a low number of objects, this condition was always satisfied in our datasets. Centroids of each mother centriole and each kinetochore were determined manually in ImageJ (NIH, Bethesda, MA, USA), and the 3D coordinates extracted in MatLab (Mathworks, Natick, MA, USA). The results were validated by superimposing the final 3D trajectories over the original time-lapse movies in an in-house written MatLab viewer. MatLab code used for visualization and analysis is available upon request.

Deviation from average position (DAP) was calculated as described in Stumpff et al. (2008). For each chromosome, DAP was calculated in a series of 5 min windows that span from −17 to −2 min prior to AO. To classify oscillating and nonoscillating chromosomes, we used a threshold DAP value of 0.4.

This threshold was chosen based on the demonstration that overexpression of the kinesin Kif18A in HeLa cells abrogates chromosome oscillation and changes DAP from 0.46 ± 0.02 to 0.31 ± 0.01(Stumpff et al., 2008).

Correlative Electron Microscopy

Cells were fixed in 2.5% glutaraldehyde (Sigma). DIC and fluorescence images were acquired at 0.1 μm Z steps through the entire cell volume immediately after fixation. Post-fixation, embedding, and sectioning were done as previously described (Rieder and Cassels, 1999). Eighty nanometer thin sections were imaged on a Zeiss 910 microscope operated at 80 kV. Scaling and alignment of LM and EM images were done manually using Photoshop. Correlation of conspicuous morphological features between DIC and EM images was used to match the orientation and Z positions for individual focal planes, and then fluorescence images were overlaid on the EM reconstruction to determine exact positions of kinetochores.

Fixation and Immunofluorescence

Cells were pre-extracted in warm PEM buffer (100 mM PIPES [pH 6.9], 2.5 mM EGTA, 5 mM $MgCl_2$) supplemented with 0.5% Triton X-100 for 1 min and fixed with 1%–2% glutaraldehyde for 10 min in PEM. Microtubules were visualized with DM1A monoclonal anti-α-tubulin antibody (Sigma). Hoechst 33343 was used to stain DNA (chromosomes).

Amira software (Visage Imaging) was used for surface rendering. To display centrioles and kinetochores in different colors, it was necessary to separate them in the imported images by masking either centrin1-GFP- or CENP-A-GFP-containing structures.

Computational Modeling

We considered the nuclear space to be an oblate spheroid with dimensions 14 μm × 14 μm × 7 μm (based on dimensions gleaned from experimental images), with 2 centrosomes at the poles of the spheroid and 46 chromosomes (92 kinetochores) inside. The chromosomes were either distributed in the nuclear space uniformly or concentrated in the ring (toroid) with inner radius 4 μm and outer radius 7 μm. The chromosome arms were allowed to slightly overlap (due to their elasticity). In the course of the simulations, the chromosomes neither moved nor rotated. Chromosomes and kinetochores were cylindrical objects with dimensions given below. During the search, each centrosome nucleated 150 microtubules in random directions, undergoing dynamic instability with the growth and shortening rates shown below. There were neither rescues nor spontaneous catastrophe events. The microtubules were undergoing a catastrophe immediately if growing outside the nuclear space or when hitting a chromosome arm; the microtubules did not turn. When a microtubule encountered a kinetochore, the microtubule was stabilized and the capture took place. Stochastic Monte Carlo simulations using this algorithm and parameters below were performed as described by Paul and coworkers (2009). The results of the simulations were obtained from running each search for 4 min (of physical, not computer time), for 100 times, and then by averaging.

Parameters Used in the Simulations

Number of chromosomes = 46; Number of microtubules from each pole = 150; kinetochore length = 0.35 μm; kinetochore diameter = 0.35 μm; chromosome diameter = 1.5 μm; chromosome length = 4 μm; microtubule growth rate = 0.35 μm/s; microtubule shortening rate = 1 μm/s.

SUPPLEMENTAL INFORMATION

Supplemental Information includes four figures and seven movies and can be found with this article online at doi:10.1016/j.cell.2011.07.012.

ACKNOWLEDGMENTS

This work was supported by NIH grants GM059363 (A.K.) and GM068952 (A.M.) and a Kirschstein National Research Service Award GM077911 to C.B.O. We acknowledge use of the Wadsworth Center's electron microscopy core facility and the Ordway Research Institute's Flow Cytometry Core. A special thanks to Dr. Duane Compton (Dartmouth Medical School) for his generous donation of anti-KID serum. V.M., C.B.O., and A.K. designed the experiments. V.M., C.B.O., and J.L. performed the experiments. R.P. and A.M. developed the computational model. V.M. designed the MatLab tools to visualize and numerically analyze kinetochore/centrosome trajectories. All authors analyzed and interpreted the data. The manuscript was written primarily by C.B.O. and A.K. with significant input from V.M. and other authors.

Received: September 30, 2010
Revised: April 17, 2011
Accepted: July 8, 2011
Published: August 18, 2011

REFERENCES

Allison, D.C., and Nestor, A.L. (1999). Evidence for a relatively random array of human chromosomes on the mitotic ring. J. Cell Biol. *145*, 1–14.

Bakhoum, S.F., Genovese, G., and Compton, D.A. (2009). Deviant kinetochore-microtubule dynamics underlie chromosomal instability. Curr. Biol. *19*, 1937–1942.

Blangy, A., Lane, H.A., d'Hérin, P., Harper, M., Kress, M., and Nigg, E.A. (1995). Phosphorylation by p34cdc2 regulates spindle association of human Eg5, a kinesin-related motor essential for bipolar spindle formation in vivo. Cell *83*, 1159–1169.

Cahu, J., Olichon, A., Hentrich, C., Schek, H., Drinjakovic, J., Zhang, C., Doherty-Kirby, A., Lajoie, G., and Surrey, T. (2008). Phosphorylation by Cdk1 increases the binding of Eg5 to microtubules in vitro and in Xenopus egg extract spindles. PLoS ONE *3*, e3936.

Cai, S., O'Connell, C.B., Khodjakov, A., and Walczak, C.E. (2009). Chromosome congression in the absence of kinetochore fibres. Nat. Cell Biol. *11*, 832–838.

Chaly, N., and Brown, D.L. (1988). The prometaphase configuration and chromosome order in early mitosis. J. Cell Sci. *91*, 325–335.

DeLuca, J.G., Moree, B., Hickey, J.M., Kilmartin, J.V., and Salmon, E.D. (2002). hNuf2 inhibition blocks stable kinetochore-microtubule attachment and induces mitotic cell death in HeLa cells. J. Cell Biol. *159*, 549–555.

DeLuca, J.G., Dong, Y., Hergert, P., Strauss, J., Hickey, J.M., Salmon, E.D., and McEwen, B.F. (2005). Hec1 and nuf2 are core components of the kinetochore outer plate essential for organizing microtubule attachment sites. Mol. Biol. Cell *16*, 519–531.

Ganem, N.J., Godinho, S.A., and Pellman, D. (2009). A mechanism linking extra centrosomes to chromosomal instability. Nature *460*, 278–282.

Goshima, G., and Vale, R.D. (2005). Cell cycle-dependent dynamics and regulation of mitotic kinesins in Drosophila S2 cells. Mol. Biol. Cell *16*, 3896–3907.

Jaqaman, K., King, E.M., Amaro, A.C., Winter, J.R., Dorn, J.F., Elliott, H.L., McClelland, S.E., Porter, I.M., Posch, M., Toso, A., et al. (2010). Kinetochore alignment within the metaphase plate is regulated by centromere stiffness and microtubule depolymerases. J. Cell Biol. *188*, 665–667.

Kapitein, L.C., Peterman, E.J., Kwok, B.H., Kim, J.H., Kapoor, T.M., and Schmidt, C.F. (2005). The bipolar mitotic kinesin Eg5 moves on both microtubules that it crosslinks. Nature *435*, 114–118.

Kapoor, T.M., Lampson, M.A., Hergert, P., Cameron, L., Cimini, D., Salmon, E.D., McEwen, B.F., and Khodjakov, A. (2006). Chromosomes can congress to the metaphase plate before biorientation. Science *311*, 388–391.

Khodjakov, A., Gabashvili, I.S., and Rieder, C.L. (1999). "Dumb" versus "smart" kinetochore models for chromosome congression during mitosis in vertebrate somatic cells. Cell Motil. Cytoskeleton *43*, 179–185.

Kirschner, M., and Mitchison, T. (1986). Beyond self-assembly: from microtubules to morphogenesis. Cell *45*, 329–342.

Kitajima, T.S., Ohsugi, M., and Ellenberg, J. (2011). Complete tracking of kinetochores reveals the error-prone nature of homologous chromosome biorientation in mammalian oocytes. Cell *146*, this issue, 568–581.

Lénárt, P., Bacher, C.P., Daigle, N., Hand, A.R., Eils, R., Terasaki, M., and Ellenberg, J. (2005). A contractile nuclear actin network drives chromosome congression in oocytes. Nature *436*, 812–818.

Levesque, A.A., and Compton, D.A. (2001). The chromokinesin Kid is necessary for chromosome arm orientation and oscillation, but not congression, on mitotic spindles. J. Cell Biol. *154*, 1135–1146.

Magidson, V., Loncarek, J., Hergert, P., Rieder, C.L., and Khodjakov, A. (2007). Laser microsurgery in the GFP era: A cell biologist's perspective. In Laser Manipulations of Cells and Tissues, M.W. Berns and K.O. Greulich, eds. (New York: Elsevier), pp. 237–266.

Maresca, T.J., and Salmon, E.D. (2010). Welcome to a new kind of tension: translating kinetochore mechanics into a wait-anaphase signal. J. Cell Sci. *123*, 825–835.

Mole-Bajer, J. (1975). The role of centrioles in the development of the astral spindle (newt). Cytobios. *13*, 117–140.

Mosgöller, W., Leitch, A.R., Brown, J.K., and Heslop-Harrison, J.S. (1991). Chromosome arrangements in human fibroblasts at mitosis. Hum. Genet. *88*, 27–33.

Nagele, R., Freeman, T., McMorrow, L., and Lee, H.Y. (1995). Precise spatial positioning of chromosomes during prometaphase: evidence for chromosomal order. Science *270*, 1831–1835.

Nezi, L., and Musacchio, A. (2009). Sister chromatid tension and the spindle assembly checkpoint. Curr. Opin. Cell Biol. *21*, 785–795.

O'Connell, C.B., Loncarek, J., Kaláb, P., and Khodjakov, A. (2009). Relative contributions of chromatin and kinetochores to mitotic spindle assembly. J. Cell Biol. *187*, 43–51.

Paul, R., Wollman, R., Silkworth, W.T., Nardi, I.K., Cimini, D., and Mogilner, A. (2009). Computer simulations predict that chromosome movements and rotations accelerate mitotic spindle assembly without compromising accuracy. Proc. Natl. Acad. Sci. USA *106*, 15708–15713.

Rieder, C.L., and Alexander, S.P. (1990). Kinetochores are transported poleward along a single astral microtubule during chromosome attachment to the spindle in newt lung cells. J. Cell Biol. *110*, 81–95.

Rieder, C.L., and Cassels, G. (1999). Correlative light and electron microscopy of mitotic cells in monolayer cultures. Methods Cell Biol. *61*, 297–315.

Rieder, C.L., and Salmon, E.D. (1994). Motile kinetochores and polar ejection forces dictate chromosome position on the vertebrate mitotic spindle. J. Cell Biol. *124*, 223–233.

Rieder, C.L., Davison, E.A., Jensen, L.C., Cassimeris, L., and Salmon, E.D. (1986). Oscillatory movements of monooriented chromosomes and their position relative to the spindle pole result from the ejection properties of the aster and half-spindle. J. Cell Biol. *103*, 581–591.

Roos, U.P. (1973). Light and electron microscopy of rat kangaroo cells in mitosis. I. Formation and breakdown of the mitotic apparatus. Chromosoma *40*, 43–82.

Rosenblatt, J. (2005). Spindle assembly: asters part their separate ways. Nat. Cell Biol. *7*, 219–222.

Silkworth, W.T., Nardi, I.K., Scholl, L.M., and Cimini, D. (2009). Multipolar spindle pole coalescence is a major source of kinetochore mis-attachment and chromosome mis-segregation in cancer cells. PLoS ONE *4*, e6564.

Skibbens, R.V., Skeen, V.P., and Salmon, E.D. (1993). Directional instability of kinetochore motility during chromosome congression and segregation in mitotic newt lung cells: a push-pull mechanism. J. Cell Biol. *122*, 859–875.

Stumpff, J., von Dassow, G., Wagenbach, M., Asbury, C., and Wordeman, L. (2008). The kinesin-8 motor Kif18A suppresses kinetochore movements to control mitotic chromosome alignment. Dev. Cell *14*, 252–262.

Tokai, N., Fujimoto-Nishiyama, A., Toyoshima, Y., Yonemura, S., Tsukita, S., Inoue, J., and Yamamota, T. (1996). Kid, a novel kinesin-like DNA binding protein, is localized to chromosomes and the mitotic spindle. EMBO J. *15*, 457–467.

Tokai-Nishizumi, N., Ohsugi, M., Suzuki, E., and Yamamoto, T. (2005). The chromokinesin Kid is required for maintenance of proper metaphase spindle size. Mol. Biol. Cell *16*, 5455–5463.

Toso, A., Winter, J.R., Garrod, A.J., Amaro, A.C., Meraldi, P., and McAinsh, A.D. (2009). Kinetochore-generated pushing forces separate centrosomes during bipolar spindle assembly. J. Cell Biol. *184*, 365–372.

Uetake, Y., and Sluder, G. (2010). Prolonged prometaphase blocks daughter cell proliferation despite normal completion of mitosis. Curr. Biol. *20*, 1666–1671.

Uteng, M., Hentrich, C., Miura, K., Bieling, P., and Surrey, T. (2008). Poleward transport of Eg5 by dynein-dynactin in Xenopus laevis egg extract spindles. J. Cell Biol. *182*, 715–726.

Walczak, C.E., Cai, S., and Khodjakov, A. (2010). Mechanisms of chromosome behaviour during mitosis. Nat. Rev. Mol. Cell Biol. *11*, 91–102.

Whitehead, C.M., Winkfein, R.J., and Rattner, J.B. (1996). The relationship of HsEg5 and the actin cytoskeleton to centrosome separation. Cell Motil. Cytoskeleton *35*, 298–308.

Wollman, R., Cytrynbaum, E.N., Jones, J.T., Meyer, T., Scholey, J.M., and Mogilner, A. (2005). Efficient chromosome capture requires a bias in the 'search-and-capture' process during mitotic-spindle assembly. Curr. Biol. *15*, 828–832.

Yang, Z., Loncarek, J., Khodjakov, A., and Rieder, C.L. (2008). Extra centrosomes and/or chromosomes prolong mitosis in human cells. Nat. Cell Biol. *10*, 748–751.